Sub Topic: Gas Turbines

Spring Technical Meeting
Eastern States Section of the Combustion Institute
March 10-13, 2024
Athens, Georgia

Effect of Diluents on Flame Stability in Constant Flame Speed Mixtures for Piloted, Swirl-Stabilized Flames

Javier Rodriguez Camacho[1] and Jacqueline O'Connor[1]*

[1]Mechanical Engineering, Pennsylvania State University, University Park, PA, USA
[*]Corresponding Author Email: jxo22@psu.edu

Abstract: This study considers the effect of exhaust gas recirculation diluents on the static and dynamic stability of a swirl-stabilized flame in a model gas turbine combustor. The test matrix is designed such that the unstretched laminar flame speed of the mixture is maintained constant as the diluent level and composition is varied. Results show that the constant flame speed test matrices exhibit similar flame stability and shape. This can be attributed to the similar stretched flame properties that these conditions exhibit when the unstretched laminar flame speed is matched.
Keywords: Carbon capture, swirl-stabilized flame, thermoacoustic instability

1. Introduction

Carbon capture for CO_2 sequestration is one option for the decarbonization of both stationary and marine power sources [1]-[3]. Although there are many carbon capture systems being pursued, they all work more efficiently if the exhaust stream has a higher concentration of CO_2 [1]-[5]. To facilitate a higher CO_2 concentration, combustion devices can use exhaust gas recirculation (EGR), where portions of the exhaust stream are mixed with incoming air to the engine. In this study, we consider the impact of the diluents found in EGR on the stability of a flame in a single-nozzle, model gas turbine combustor.

A typical gas turbine engine is operated a constant turbine inlet temperature to maintain the life of the hot-section components. As such, our previous EGR studies have considered the impact of diluents on flame stability using a test matrix with a constant adiabatic flame temperature [6]. These results showed that decreasing the oxygen concentration in the reactants generally reduced static flame stability and had a non-monotonic effect on the amplitude and characteristics of dynamic flame oscillations. However, our previous findings have also shown that the flame stability is largely dependent on the flame speed, rather than flame temperature. In this study, we use a constant flame speed test matrix to understand the impact of diluents on flame static and dynamic stability in an industry-relevant, single-nozzle combustor.

2. Methods / Experimental

Experiments were completed in a single-nozzle, central-piloted, swirl-stabilized combustion experiment with a variable-length exhaust that allows for significant variation in the acoustic modes of the combustor. Figure 1 shows the schematic of the experiment, which is described in more detail in Rodriguez Camacho et al. [6]. A dynamic pressure transducer located in the dump plane was used to determine the dynamic stability of the combustor and high-speed CH* chemiluminescence imaging was used to image the shape and dynamics of the natural gas flame.

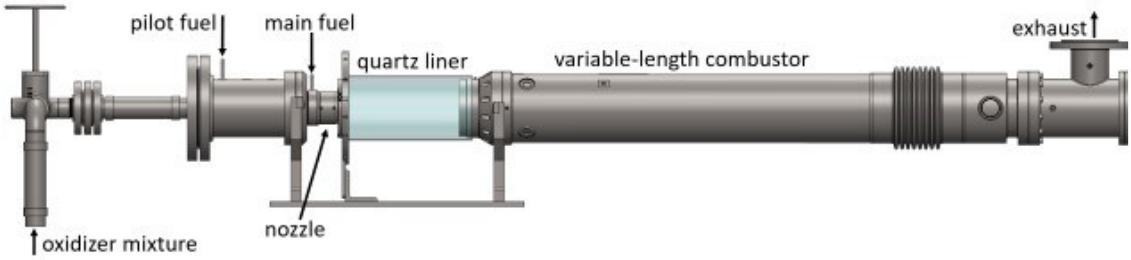

Figure 1. Experimental combustor rig showing relevant components and reactant streams.

3. Results and Discussion

Table 1 shows the test matrix considered in this study, where three different unstretched laminar flame speeds (S_L^0) – 38.34 cm/s, 20.32 cm/s, and 15.63 cm/s – were obtained by varying the equivalence ratio at a constant inlet temperature of 250 °C and several different compositions of diluent gases. The conditions, shown in Figure 2, were calculated using Chemkin Pro [7] with the GRIMech 3.0 [8]. The conditions are tested with a neutral pilot, where the main and pilot flame have the same equivalence ratio.

Table 1. Test matrix for three different unstretched laminar flame speeds

Condition	O_2	CO_2	N_2	ϕ	S_L^o [cm/s]
Baseline_SL1	0.21	0	0.79	0.57	38.34
C19_SL1	0.19	0.03	0.78	0.67	38.54
C17_SL1	0.17	0.08	0.75	0.86	38.41
N17_SL1	0.17	0.05	0.78	0.806	38.34
Baseline_SL2	0.21	0.00	0.79	0.47	20.32
C19_SL2	0.19	0.03	0.78	0.541	20.32
C17_SL2	0.17	0.08	0.75	0.653	20.32
C15_SL2	0.15	0.12	0.73	0.824	20.32
N17_SL2	0.17	0.05	0.78	0.63	20.32
N15_SL2	0.15	0.07	0.78	0.759	20.32
Baseline_SL3	0.21	0.00	0.79	0.44	15.63
C19_SL3	0.19	0.03	0.78	0.505	15.63
C17_SL3	0.17	0.08	0.75	0.603	15.63
C15_SL3	0.15	0.12	0.73	0.741	15.63
N17_SL3	0.17	0.05	0.78	0.583	15.63
N15_SL3	0.15	0.07	0.78	0.693	15.63

Figure 3 shows the top half of the time-averaged, Abel-inverted flame shape for all cases, with flow moving from left to right and the centerline located at the bottom of each image. The top left image has a sketch of the nozzle section, including the location of the centerbody, pilot jet, annular jet, dump plane, centerline, and combustor wall. At the higher flame speed conditions, the flame is stabilized in a V-flame configuration. The maximum unstretched laminar flame speeds for C15 and N15 are approximately 27 cm/s and 33 cm/s respectively. At the highest flame speed condition, there is no equivalence ratio at which the N15_SL1 and C15_SL1 conditions can reach the SL1 flame speed and so are not tested. As flame speed is decreased the flame images show an increase

in flame length with the flame extending into the metallic section of the experimental rig. Additionally, as the flame speed decreases the flame becomes less compact and covers a larger volume of the combustor. Furthermore, at the lowest flame speed tested, none of the conditions show flame activity in the corner recirculation region of the combustor. At the lowest flame speed condition, the flame is close to blowout, however the C19_SL3 condition is the only flame that cannot be stabilized and results in immediate blowout after ignition. The remaining SL3 conditions experience some degree of blowout at the long combustor lengths.

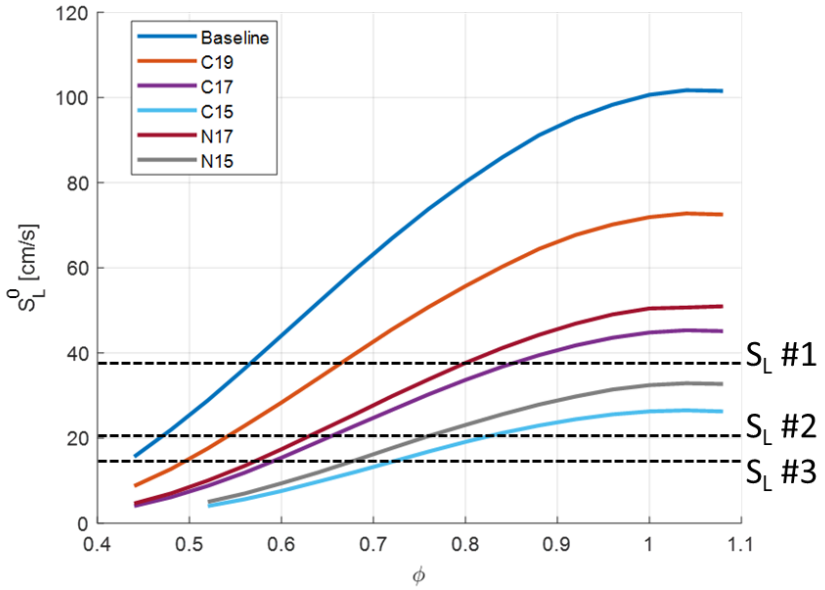

Figure 2. Unstretched laminar flame speed for the EGR mixtures of interest showing the three flame speeds tested.

The general change in flame stabilization at different conditions is a result of the lower flame speeds and the decreased extinction strain rates that the flame can sustain. However, by matching the unstretched laminar flame speed the stretched flame behavior is similar for all test conditions. The stretched laminar flame speeds for the SL1 conditions are shown in Figure 4 to illustrate the trend within test groups. This behavior repeats itself for the SL2 and SL3 conditions. Due to the similar unstretched and stretched flame properties the flame shapes and the general static stability of the flame is similar within each test group. This behavior is somewhat observed for the dynamic stability of the flame.

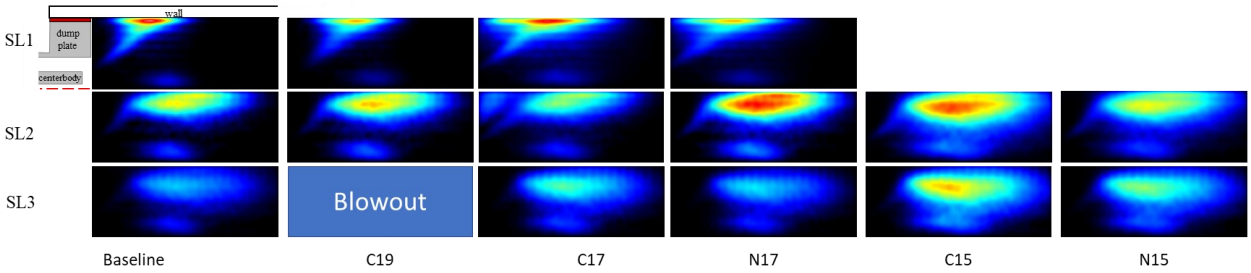

Figure 3. Top half of time-averaged, Abel-inverted flame shape for all test conditions at a combustor length of 25 inches. Top left image includes a schematic of the nozzle section.

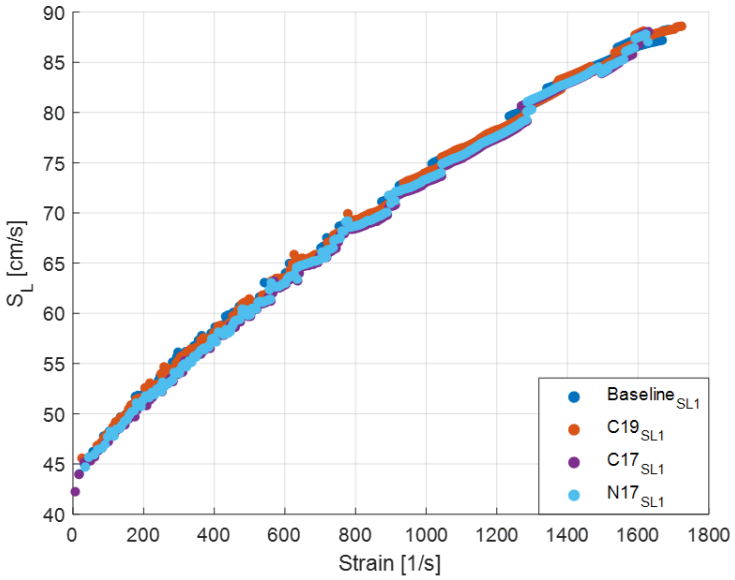

Figure 4. Stretched flame behavior for the SL1 test conditions.

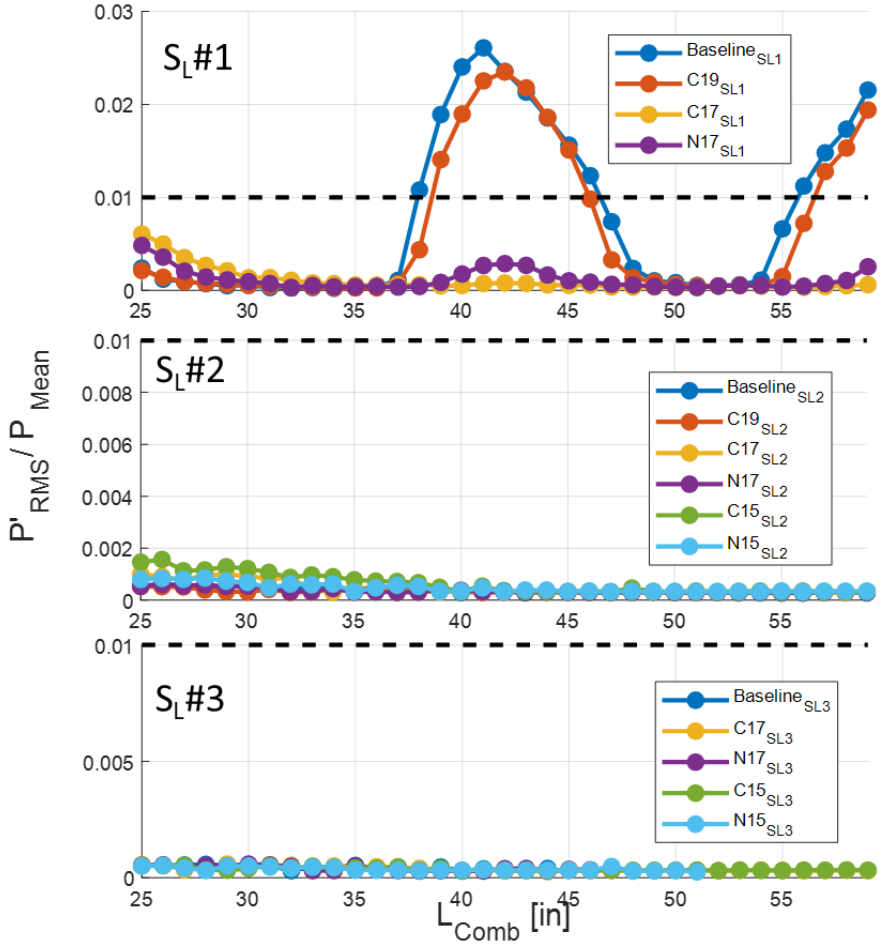

Figure 5. Dynamic stability maps of the combustor as a function of combustor length - stability threshold denoted by the dashed black line.

Figure 5 shows the combustor pressure fluctuation amplitude as a function of combustor length for all the test conditions. This combustor typically has three instability modes as a function of combustor length – 25” (~170 Hz), 42” (~370 Hz), and 59” (~220 Hz) [6]. The SL1 conditions show a change in stability as the level of dilution increases. At the higher oxygen conditions the system is unstable around 42” and 59”. Increasing the diluents, for C17_SL1 and N17_SL1, results in the system becoming stable for all combustor lengths. The SL2 and SL3 test conditions exhibit similar dynamic stability within their respective groups, with all conditions stable with respect to the stability threshold. The flame stability is likely a result of the flame lifting from the shear layer separation point downstream of the centerbody, which had been shown to suppress instability in a previous study [6].

4. Conclusions

A constant flame speed test matrix was evaluated for an EGR-diluted natural gas flame. Static and dynamic stability show similar behavior within each flame speed group. The use of stretched flame properties can be used to evaluate flame stability for flames with different oxidizer compositions. Additional parameters might be necessary to adequately determine flame stability, as in the case of the SL1 test matrix where there are two different behaviors. Further testing will look at the effect of hydrogen addition on flame stability for EGR diluted flames.

5. Acknowledgements

The authors would like to acknowledge funding by the National Science Foundation under grant CBET-1749679 as well as ONR Grant N00014-23-1-2725 with program monitor Mark Spector.

6. References

[1] Songolzadeh, M., Soleimani, M., Takht Ravanchi, M., & Songolzadeh, R. (2014). “Carbon dioxide separation from flue gases: A technological review emphasizing reduction in greenhouse gas emissions,” The Scientific World Journal, p. 828131.

[2] Zamarripa, M. A., Eslick, J. C., Matuszewski, M. S., & Miller, D. C. (2018). “Multi-objective optimization of membrane-based CO2 capture” In: 13 International Symposium on Process Systems Engineering (PSE 2018), Vol. 44, pp. 1117–1122.

[3] Hasan, M. M. F., Baliban, R. C., Elia, J. A., & Floudas, C. A. (2012). “Modeling, simulation, and optimization of post-combustion CO2 capture for variable feed concentration and flow rate. 1. Chemical absorption and membrane processes.” Industrial & Engineering Chemistry Research, Vol. 51, No. 48, p. 15642–15664.

[4] Burnes, D., & Saxena, P. (2022). “Operational scenarios of a gas turbine using exhaust gas recirculation for carbon capture.” Journal of Engineering for Gas Turbines and Power, Vol. 144, No. 2, p. 1–12.

[5] Burnes, D, Saxena, P, & Dunn, P. (2020). “Study of using exhaust gas Recirculation on a gas turbine for carbon capture.” ASME Turbo Expo, Virtual, Online.

[6] Rodriguez Camacho, J., Akiki, M., Blust, J., and O'Connor, J. (January 12, 2024). "Effect of Inert Species on the Static and Dynamic Stability of a Piloted, Swirl-Stabilized Flame." ASME. J. Eng. Gas Turbines Power. June 2024; 146(6): 061021. https://doi.org/10.1115/1.4064048

[7] R. J. Kee et al., “Ansys Chemkin-Pro 2022 R1.” 2022.

[8] Smith, G.P., Golden, D.M., Frenklach, M., Moriarty, M.W., Eiteneer, B., Goldenberg, M., Bowman, C.T., Hanson, R.K., Song, S., Gardiner, Jr., W.C., Lissianski, V.V., & Qin, Z. “GRIMech 3.0,” http://www.me.berkeley.edu/gri_mech/